Ruthenium-mediated selective cleavage of nitrogen–carbon bond of the diimine function. Synthesis, spectroscopic and redox properties of the complexes $[Ru(L)_2\{^-OC_6H_4C(CH_3)=N-H\}][ClO_4]$ (L = 2,2′-bipyridine and 1,10-phenanthroline) and the crystal structure of the bipyridine derivative

Soma Chakraborty, Mrinalini G. Walawalkar, Goutam Kumar Lahiri *

Department of Chemistry, Indian Institute of Technology, Bombay, Powai, Mumbai 400 076, India

Abstract

The reactions of $Ru(bpy)_2(CO_3)$ (bpy = 2,2′-bipyridine) and $Ru(phen)_2(CO_3)$ (phen = 1,10-phenanthroline) with the binucleating phenolato diimine function, $OH–C_6H_4–C(CH_3)=N–CH_2–C_6H_4–CH_2–N=(CH_3)C–C_6H_4–OH$, H_2L in ethanol solvent under dinitrogen atmosphere result in ruthenium bipyridine/phenanthroline heterochelates $[Ru(bpy)_2/(phen)_2L'](ClO_4)$ **1** where L′ corresponds to the ketonic imine function $^-O–C_6H_4C(CH_3)=N–H$ incorporating the rare >C=N–H fragment. In the course of the reaction the N–C bond of the diimine function in H_2L has been selectively cleaved. The formation of **1** has been authenticated by single-crystal X-ray structure of the bipyridine derivative (**1a**). The RuN_5O coordination sphere is distorted octahedral. The diamagnetic complexes **1** exhibit 1:1 conductivity in acetonitrile solution. The complexes show strong $Ru^{II} \rightarrow \pi^*$(bpy)/(phen) MLCT transitions in the visible region and intra-ligand transitions in the UV region. The complexes exhibit moderately strong emissions near 700 nm from the lowest energy MLCT bands ($\Phi = 1.7–2.2 \times 10^{-2}$). The complexes (**1a** and **1b**) display reversible ruthenium(III)–ruthenium(II) couple near 0.5 V, irreversible ruthenium(III) → ruthenium(IV) oxidation near 1.7 V and one ligand-based (L′) oxidation near 2.0 V versus SCE. The reductions of the bpy and phen ligands have been observed at the negative side of SCE. The electrochemically oxidized ruthenium(III) complexes ($\mathbf{1a}^+$ and $\mathbf{1b}^+$) are found to be unstable at 298 K and exhibit rhombic EPR spectra having three distinct *g* values corresponding to the trivalent ruthenium(III) under distorted octahedral arrangement. The oxidized complexes ($\mathbf{1a}^+$ and $\mathbf{1b}^+$) exhibit LMCT transitions near 750 nm.

Keywords: Diimine function; Redox properties; Spectroscopic properties

1. Introduction

Metal ion mediated transformation of organic molecules is known to be a fundamentally important chemical process [1,2]. This may lead to the formation of important molecules which are otherwise difficult or even impossible to synthesize by following the conventional routes [3–8]. In this process the metal ion acts as a pivot, which provides a suitable chemical platform in directing the reaction equilibrium. In recent years we have observed the effective role of ruthenium, osmium, cobalt and rhenium complexes in catering the unusual and selective organic transformations [9–19]. In this article we wish to report a reaction where the N–C bond of the binucleating bridging ligand, $OH–C_6H_4–C(CH_3)=N–CH_2–C_6H_4–CH_2–N=(CH_3)C–C_6H_4–OH$, H_2L has been selectively and directly cleaved in the presence of ruthenium starting complexes $[Ru(bpy)_2CO_3]$ and $[Ru(phen)_2CO_3]$ (bpy = 2,2′-bipyridine and phen = 1,10-phenanthroline) [19]. Although our primary intention was to develop the binuclear ruthenium–bipyridine and phenanthroline complexes by using the phenolato imine based bridging ligand H_2L as a possible photo-redox assembly, the reactions in

turn lead to the formation of mononuclear ruthenium–bipyridine/phenanthroline derivatives $[Ru(bpy)_2/(phen)_2L']^+$ 1, where L′ corresponds to the ketonic imine function $^-O–C_6H_4–C(CH_3)=N–H$ incorporating rare $^-C(CH_3)=N–H$ fragment via the cleavage of N–C bond of H_2L.

Herein we report the synthesis, a comparative spectroscopic and redox properties of the complexes (**1a** and **1b**) and crystal structure of the bipyridine derivative (**1a**).

2. Experimental

2.1. Materials

The starting ruthenium complexes, $Ru(bpy)_2CO_3$ and $Ru(phen)_2CO_3$ were prepared by following the reported procedure [20]. 2-Hydroxyacetophenone and α,α′-diamino-*p*–xylene were obtained from Fluka, Switzerland. Other chemicals and solvents were of reagent grade and used as received. Silica gel (60–120 mesh) used for chromatography was of BDH quality. For spectroscopic and electrochemical studies HPLC grade solvents were used. Commercial tetraethyl ammonium bromide was converted into pure tetraethyl ammonium perchlorate by following an available procedure [21].

2.2. Physical measurements

Solution electrical conductivity was checked using Systronic-305 conductivity bridge. Magnetic susceptibility was checked with the PAR vibrating-sample magnetometer. UV–Vis spectra were recorded by using a Shimadzu 2100 spectrophotometer. FT-IR spectra were taken on a Nicolet spectrophotometer with samples prepared as KBr pellets. NMR spectra were obtained with a 300 MHz Varian FT spectrometer. Cyclic voltammetric, differential pulse voltammetric and coulometric measurements were carried out using a PAR model 273A electrochemistry system. A platinum working electrode, platinum auxiliary electrodes and a saturated calomel reference electrode (SCE) were used in a three-electrode configuration. The supporting electrolyte was $[NEt_4][ClO_4]$ and the solute concentration was $\sim 10^{-3}$ M. The half-wave potential E°_{298} was set equal to $0.5(E_{pa} + E_{pc})$, where E_{pa} and E_{pc} are anodic and cathodic cyclic voltammetric peak potentials, respectively. A platinum wire gauze working electrode was used in coulometric experiments. All experiments were carried out under a dinitrogen atmosphere and were uncorrected for junction potentials. The elemental analyses were carried out with Carlo Erba elemental analyzer. The EPR measurements were made with a Varian model 109C E line X-band spectrometer fitted with a quartz Dewar for measurements at 77 K (liquid nitrogen). The spectra were calibrated by using tetracyanoethylene (tcne) radical ($g = 2.0023$). Solution emission properties were checked using a SPEX fluorolog spectrofluorometer.

2.3. Preparation of the ligand H_2L and the complexes (**1a** and **1b**)

2.3.1. $OH–C_6H_4–C(CH_3)=N–CH_2–C_6H_4–CH_2–N=(CH_3)C–C_6H_4–OH$, H_2L

The ligand $OH–C_6H_4–C(CH_3)=N–CH_2–C_6H_4–CH_2–N=(CH_3)C–C_6H_4–OH$ (H_2L) was prepared by condensing 2-hydroxyacetophenone (0.99 g, 7.25 mmol) with α,α′-diamino-*p*–xylene (0.49 g, 3.63 mmol) in a 2:1 mol ratio in dry ethanol under stirring condition at room temperature (r.t.). The solid product thus obtained was then filtered and dried under vacuum. The crude product was then recrystallized from hot ethanol. Yield: 1.15 g (85%).

The complexes $[Ru(bpy)_2L'](ClO_4)$ (**1a**) and $[Ru(phen)_2L'](ClO_4)$ (**1b**) were prepared by following a general procedure. Details are mentioned for **1b**.

2.3.2. $[Ru(phen)_2L'](ClO_4)$ (**1b**)

The starting complex, $Ru(phen)_2CO_3$ (0.30 g, 0.57 mmol) was dissolved in ethanol (25 ml).The ligand H_2L (0.106 g, 0.285 mmol) and anhydrous sodium acetate (0.047 g, 0.57 mmol) were then added to the above metal solution. The resulting mixture was heated to reflux under N_2 atmosphere overnight. After this the volume of the solution was reduced and a saturated aqueous solution (5 ml) of $NaClO_4$ was added and then cooled. The precipitate thus formed was filtered and washed thoroughly with cold ethanol followed by ice-cold water. The product was purified by column chromatography using a silica gel column. Initially the excess ligand was eluted with benzene. The complex **1b** was separated as a dark band by acetonitrile–dichloromethane (1:5) mixture. On removal of solvent pure product was obtained in the solid state. Finally, the product was recrystallized from acetonitrile–benzene (1:3 v/v) mixture. Yield: 0.28 g (70%).

2.4. X-ray structure determination

Single crystals of the complex **1a** were grown by slow diffusion of hexane in a dichloromethane solution of **1a** followed by slow evaporation. X-ray data were collected on a Nonius MACH 3 four-circle diffractometer (graphite-monochromatized Mo Kα radiation). Significant crystal data and data collection parameters are listed in Table 1. Absorption correction was done by performing psi-scan measurement [22]. The structure was solved by using the SHELXS-93 and refined by using SHELXL-97 [23]. The metal atom was located from the Patterson map and the other non-hydrogen atoms

Table 1
Crystallographic data for $[Ru(bpy)_2L']ClO_4 \cdot C_6H_{14}$ (**1a**)

Empirical formula	$C_{34}H_{38}N_5O_5ClRu$
Formula weight	733.21
Crystal symmetry	triclinic
Space group	$P\bar{1}$
Unit cell dimensions	
a (Å)	9.643(14)
b (Å)	12.434(3)
c (Å)	14.250(3)
α (°)	107.670(19)
β (°)	94.717(14)
γ (°)	109.341(14)
V (Å^3)	1504.1(5)
Z	2
D_{calc} (g cm^{-3})	1.619
μ (mm^{-1})	0.664
R_1	0.0379
WR_2	0.1012

emerged from successive Fourier synthesis and the structure was refined by full-matrix least-squares on F^2. All non-hydrogen atoms were refined anisotropically. Hydrogen atoms were included in calculated positions.

3. Results and discussion

The phenolatoimine-based binucleating bridging ligand, H_2L has been prepared by reacting α,α′-diamino-*p*-xylene with the 2-hydroxyacetophenone in a ratio of 1:2 in dry ethanol. The pure crystalline product has been obtained in high yield (85%). The microanalytical data of the ligand match well with the calculated values (Table 2). The IR spectrum of H_2L displays one broad band at 3420 cm^{-1} due to –OH function and a sharp band at 1640 cm^{-1} due to the $-(CH_3)C{=}N-$ vibration. The ^{1}H NMR spectrum of H_2L in $CDCl_3$ solvent is shown in Fig. 1(a) and it indicates that each half of the molecule is equivalent due to internal symmetry [24]. The ligand, H_2L displays strong transitions in the UV region due to n–π* and π–π* transitions (Table 2, Fig. 2(a)) [25].

The reactions of H_2L with the starting ruthenium bipyridine and phenanthroline complexes, $Ru(bpy)_2(CO_3)$ and $Ru(phen)_2(CO_3)$ in ethanol and in presence of sodium acetate under dinitrogen atmosphere for 12 h result in dark colored solid products on addition of saturated aqueous $NaClO_4$. Chromotographic purifications of the crude products using silica gel column yield pure compounds of the composition $[Ru^{II}(bpy)_2(L')][ClO_4]$ (**1a**) and $[Ru^{II}(phen)_2(L')][ClO_4]$ (**1b**) (Scheme 1). In complexes **1a** and **1b**, L′ corresponds to the transformed ligand $^-OC_6H_4C(CH_3){=}N-H$ incorporating the rare $-(CH_3)C{=}N-H$ fragment. The binucleating form of the ligand H_2L has been found to be stable enough both in the solid and solution states. Under identical reaction conditions (Scheme 1) but in the absence of ruthenium starting complexes, $Ru(bpy)_2(CO_3)$ and $Ru(phen)_2(CO_3)$ the binucleating identity of H_2L remains intact. This implies the direct involvement of the metal fragment, $Ru(bpy)_2$ or $Ru(phen)_2$ core in facilitating the conversion of $H_2L \rightarrow L'$ in **1**.

The complexes (**1**) provide satisfactory microanalytical data (Table 2) and are diamagnetic (Ru^{II}, t_{2g}^6; $S = 0$). They exhibit 1:1 conductivity in acetonitrile solution (Table 2). The vibrational frequency due to the N–H

Table 2
Microanalytical [a], electronic spectral [b], conductivity [b] and emission [c] data

Compd.	Elemental analysis (%)			UV–Vis λ (nm) (ε (M^{-1} cm^{-1}))	Λ_M (Ω^{-1} cm^2 M^{-1})	Emission, λ_{max} (nm)		Φ
	C	H	N			Excitation	Emission	
H_2L	76.81 (77.42)	6.87 (6.45)	7.10 (7.53)	400 (1820), 322 (6650), 256 (19 460) [d]				
1a	51.88 (51.97)	3.67 (3.71)	10.95 (10.83)	574 (5500), 507 (8500), 375 (9300), 295 (46 950), 245 (32 800), 194 (49 900)	148	506	703	2.2×10^{-2}
1b	55.97 (55.28)	3.44 (3.46)	10.63 (10.08)	558 (5340), 470 (9220), 265 (54 124), 222 (54 120)	155	554	668	1.7×10^{-2}
1a$^+$				748, 373, 302, 271, 238, 195				
1b$^+$				774, 380, 270, 230				

[a] Calculated values are in parentheses.
[b] In acetonitrile.
[c] In MeOH–EtOH (1:4) glass at 77 K.
[d] In chloroform.

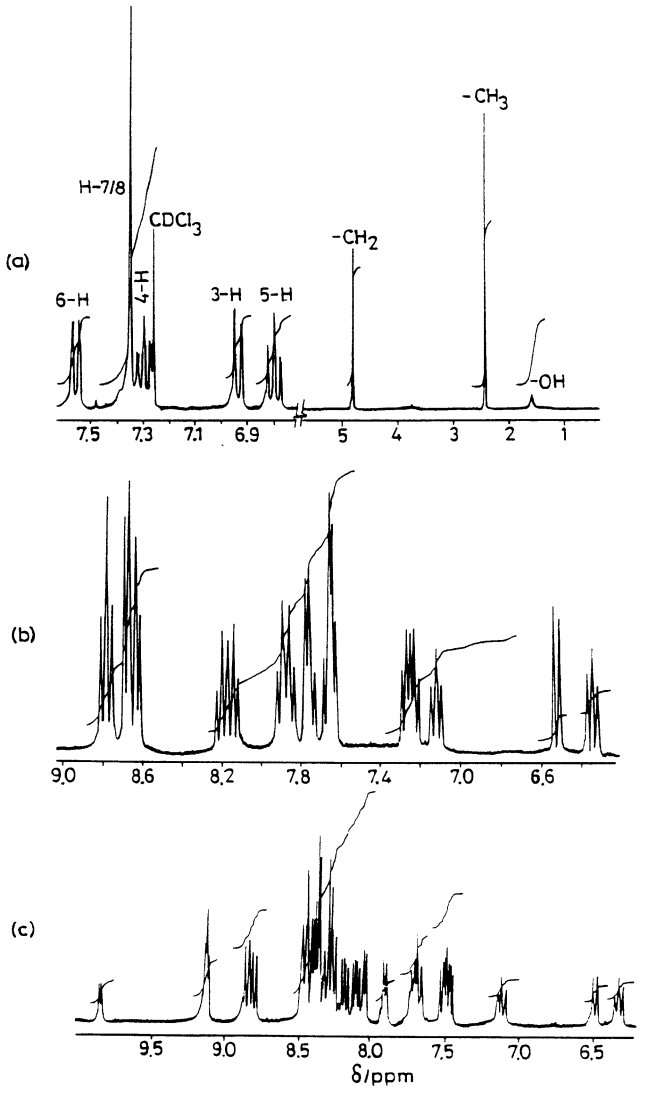

Fig. 1. ^{1}H NMR spectra of: (a) H_2L in $CDCl_3$; (b) aromatic region of complex **1a**; and (c) aromatic region of complex **1b** in $(CD_3)_2SO$.

bond in the coordinated imine fragment of L′ has been observed at 3310 cm^{-1} [26]. The vibrations due to perchlorate anion and the imine function ($\nu_{C=N}$) of the coordinated L′ have been observed at 1100/630 and 1640 cm^{-1}, respectively [27–29].

The formation of complexes **1** have been authenticated in case of bipyridine complex by the single crystal X-ray structure of **1a**. The crystal structure of **1a** is shown in Fig. 3. Selected bond distances and angles are listed in Table 3. The complex **1a** is monomeric and the lattice consists of one type of molecule where the imine function (L′) is in the bidentate mode, coordinating through its oxygen and nitrogen atoms.

The single crystal of **1a** contains hexane of crystallization in the ratio $[Ru(bpy)_2L']ClO_4:C_6H_{14} = 1:1$. The hexane molecule is distorted in the lattice. The RuN_5O coordination sphere is a distorted octahedral as can be seen from the angles subtended at the metal. Distortion from the ideal geometry is primarily due to the customary N–Ru–N bite angles of the bpy ligands [average, 79.02(12)°] and N(1)–Ru–O(1) bite angle of the imine function [88.95(10)°]. The *trans* angles, N(1)–Ru–N(2), N(3)–Ru–N(5) and O(1)–Ru–N(4) are close to 175°. The Ru^{II}–O distance is observed to be 2.060(3) Å which

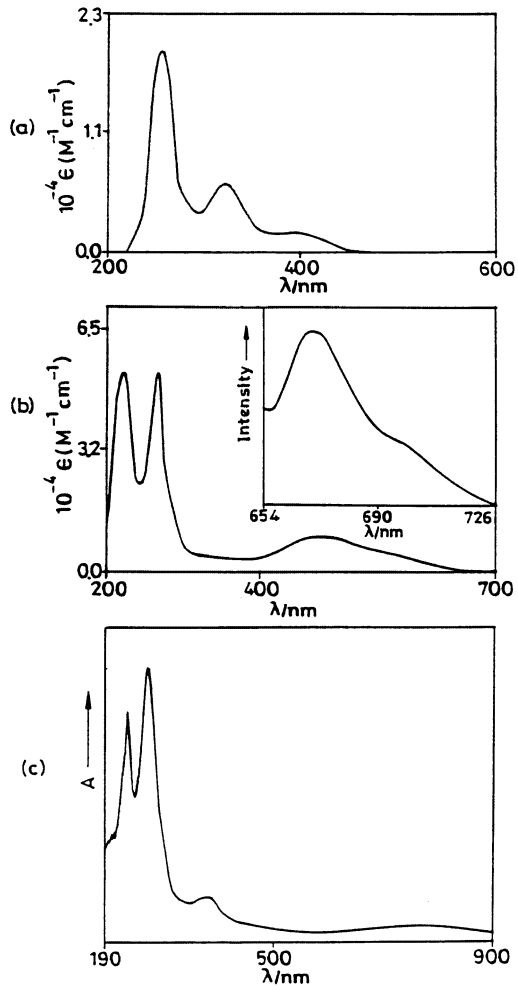

Fig. 2. Electronic spectra of: (a) H_2L in $CDCl_3$; (b) complex **1b**; and (c) coulometrically generated $\mathbf{1b}^+$ in acetonitrile.

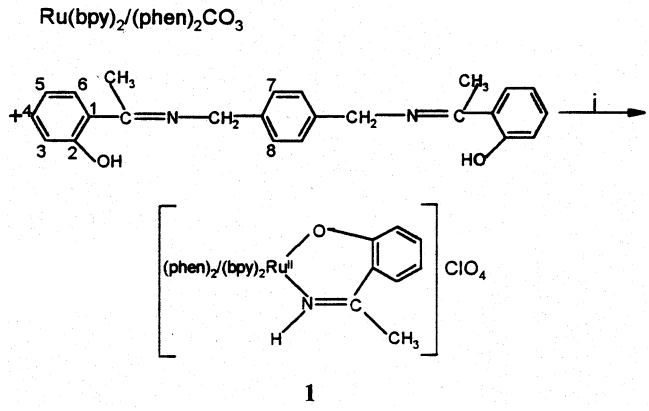

Scheme 1. (i) Ethanol, CH_3COONa, N_2, stir, $NaClO_4$.

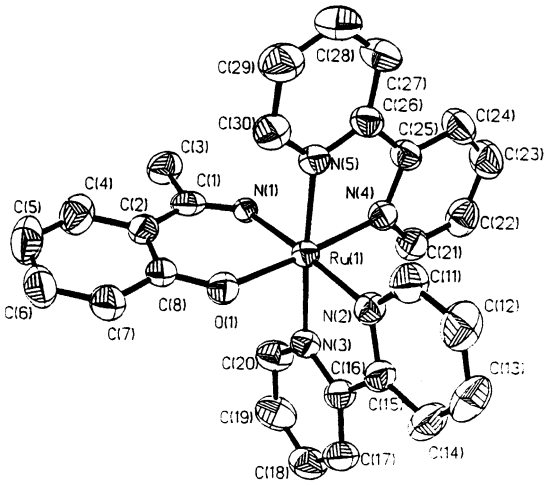

Fig. 3. Crystal structure of complex **1a**.

Table 3
Selected bond lengths (Å) and angles (°) for **1a**

Bond lengths	
Ru–N(1)	2.050(2)
Ru–N(2)	2.017(3)
Ru–N(3)	2.047(3)
Ru–N(4)	2.034(3)
Ru–N(5)	2.056(3)
Ru–O(1)	2.063(3)
C(1)–N(1)	1.240(5)
Bond angles	
N(2)–Ru–N(4)	89.63(12)
N(2)–Ru–N(3)	79.10(12)
N(4)–Ru–N(3)	97.81(12)
N(2)–Ru–N(1)	175.11(11)
N(4)–Ru–N(1)	90.69(11)
N(3)–Ru–N(1)	96.02(11)
N(2)–Ru–N(5)	97.09(12)
N(4)–Ru–N(5)	78.94(12)
N(3)–Ru–N(5)	175.07(11)
N(1)–Ru–N(5)	87.76(11)
N(2)–Ru–O(1)	91.14(11)
N(4)–Ru–O(1)	175.08(10)
N(3)–Ru–O(1)	87.11(11)
N(1)–Ru–O(1)	89.95(10)
N(5)–Ru–O(1)	96.14(11)

agrees well with the Ru^{II}–O (phenolato) distance, 2.064 (4) Å observed in $[Ru^{II}(bpy)_2(pyridine\text{-}phenol)]^+$ complex [30] but is slightly longer than the Ru^{II}–O (phenolato) distances, 2.022 (5) and 2.042(4) Å observed in $[Ru^{II}(m\text{-}tap)_2(catecholate)]$ [31] and $[Ru^{II}(bpy)_2(salicylate)]$ [32], respectively. However, it is much shorter than the Ru^{II}–O distances found in Ru^{II}–O(phenolato) in four-membered metallocycles, 2.235(4) Å [17] and 2.205(16) Å [16].

The Ru–N(bpy) bond lengths lie in the range 2.017–2.056 Å which match well with the limit of Ru–N(bpy) distances (2.0–2.12 Å) reported earlier [12,32]. The Ru–N(1) (imine nitrogen) bond length in **1a** is 2.050(2) Å. The bond distance of C(1)–N(1) is 1.240(5) Å, which is normal for a C=N double bond. The ClO_4^- is tetrahedral with an average Cl–O bond distance of 1.409(4) Å and average O–Cl–O angle of 109.48(3)°.

The ^1H NMR spectra of **1a** and **1b** in $CDCl_3$ are shown in Fig. 1. The absence of the OH-proton of free H_2L in the spectra of **1** indicates the metallation through the phenolato oxygen center. The asymmetric nature of L makes all the five aromatic rings non-equivalent. Therefore, the aromatic region of the spectra is complicated due to overlapping of several signals. However, the direct comparisons of the intensity of the aromatic region proton signals with that of the clearly observable methyl protons in the upfield region (δ 2.31 ppm for **1a** and 2.44 ppm for **1b**) reveal the presence of calculated number of aromatic protons for both the complexes [33]. The NH proton appears at δ 15.87 ppm for **1a** and δ 16.2 ppm for **1b** and disappears on D_2O treatment as expected [34].

In acetonitrile solvent the complexes (**1a** and **1b**) display $Ru(II) \rightarrow \pi^*(bpy)/(phen)$ MLCT transitions near 500 nm and intra ligand transitions in the UV region (Table 2, Fig. 2) [12,35]. In the case of phenanthroline complex, **1b** the MLCT transition is observed to be blue shifted as compared to the bipyridine analogue (**1a**).

Excitations of **1a** and **1b** at the lowest energy MLCT bands in 1:4 MeOH–EtOH glass at 77 K result in moderately strong emissions near 700 nm (Table 2, Fig. 2(b)). The quantum yields (Φ) of the emission processes were determined with respect to the quantum yield of $[Ru(bpy)_3]^{2+}$ in 1:4 MeOH–EtOH glass at 77 K (Φ = 0.35) [36] by using the earlier reported procedures [37–39]. The calculated quantum yields for the complexes are listed in Table 2. The quantum yield (Φ) data suggest that the emission efficiency of bipyridine (**1a**) and phenanthroline (**1b**) complexes are comparable.

The redox properties of the complexes (**1a** and **1b**) have been recorded in acetonitrile solvent using platinum working electrode. The reduction potential data are listed in Table 4 and the representative voltammograms are shown in Fig. 4. The complexes exhibit three successive one-electron oxidative responses at the positive side of SCE and two one-electron reductions at the negative side of SCE. The observed reversible oxidative process near 0.5 V (couple-I, Fig. 4) is assigned to be the ruthenium(III)–ruthenium(II) couple [40].

The one-electron nature of the couple has been confirmed by constant potential coulometry (Table 4). The coulometric oxidations of the complexes (**1a** and **1b**) at 0.7 V generate green colored oxidized species. The resulting oxidized solution shows cyclic voltammograms which are superimposable to those of the starting bivalent complexes, $[Ru^{II}(bpy)_2(L')][ClO_4]$ (**1a**) and $[Ru^{II}(phen)_2(L')][ClO_4]$ (**1b**).This implies the stereoretentive nature of the oxidation process. The oxidized

Table 4
Electrochemical data at 298 K [a] and EPR g values in acetonitrile at 77 K

Compound	E°_{298} (V) (ΔE_p (mV))						g_1	g_2	g_3
	Ru^{III}–Ru^{II} (couple-I)	n [b]	$Ru^{III} \rightarrow Ru^{IV}$ (couple-II)	Ligand oxidation (couple-III)	Ligand reduction				
					Couple-IV	Couple-V			
1a	0.52 (80)	1.09	1.71 [c]	2.25 [c]	−1.56 (70)	−1.79 (100)	2.333	2.061	1.867
1b	0.49 (60)	1.11	1.63 [c]	2.01 [c]	−1.59 (78)	−1.83 (120)	2.439	2.101	1.823

[a] Conditions: solvent, acetonitrile; supporting electrolyte, NEt_4ClO_4; reference electrode, SCE; solute concentration, $\sim 10^{-3}$ M; working electrode, platinum. Cyclic voltammetric data: scan rate, 50 mV s^{-1}; $E^{\circ}_{298} = 0.5(E_{pc} + E_{pa})$ where E_{pc} and E_{pa} are the cathodic and anodic peak potentials, respectively.

[b] $n = Q/Q'$ where Q' is the calculated Coulomb count for $1e^-$ transfer and Q that found after exhaustive electrolysis of $\sim 10^{-2}$ M solute.

[c] E_{pa} is considered due to irreversible nature of the voltammograms.

solution can be quantitatively reduced to the parent bivalent state. The oxidized green complexes $\mathbf{1a}^+$ and $\mathbf{1b}^+$ are unstable at room temperature; however, we have managed to record the EPR spectra of $\mathbf{1}^+$ by quickly freezing the oxidized solutions in liquid nitrogen (77 K). The presence of trivalent ruthenium ion in the oxidized solutions has been confirmed by the characteristic rhombic EPR spectra of the ruthenium(III) species under distorted octahedral arrangement (Table 4) [41]. The qualitative absorption spectral data of $\mathbf{1a}^+$ and $\mathbf{1b}^+$ are listed in Table 2 and the spectrum of $\mathbf{1b}^+$ has been displayed in Fig. 2(c). The complexes exhibit $\pi(bpy)/(phen) \rightarrow t_{2g}$ (Ru^{III}) LMCT transitions near 750 nm and intraligand transitions in the UV region (Table 2) [30].

The ruthenium(III)–ruthenium(II) potential decreases by 30 mV on moving from the bipyridine (**1a**) to the phenanthroline (**1b**) environment. On the other hand, replacement of one π-acidic bpy or phen function from the $[Ru(bpy)_3]^{2+}$ or $[Ru(phen)_3]^{2+}$ by the σ-donating L′ in the complex **1** decreases the ruthenium(III)–ruthenium(II) potential appreciably. This is due to the reduction of overall charge of the complex cation from $+2$ in $[Ru(bpy)_3]^{2+}$ and $[Ru(phen)_3]^{2+}$ to $+1$ in **1** which provides electrostatic stabilization of the oxidized Ru^{III}–L′ species.

The chemical oxidations of the complexes **1a** and **1b** by using aqueous ammonium cerium(IV) sulfate or ammonium cerium(IV) sulfate in 0.1 M aqueous $HClO_4$ also result in unstable green colored oxidized species ($\mathbf{1a}^+$ and $\mathbf{1b}^+$).

The complexes display a second irreversible oxidation process in the range 1.6–1.7 V (couple-II, Fig. 4).The one-electron nature of the process has been established by comparing its differential pulse voltammetric current height with that of the previous reversible ruthenium(III)–ruthenium(II) couple. Based on the separation between the two successive oxidation processes (couple-II–couple-I, ~ 1.3 V, Table 4, Fig. 4) the second oxidation process may be considered to be ruthenium(III) → ruthenium(IV) oxidation [42,43].

The complexes exhibit one more one-electron irreversible oxidation process near 2.2 V (couple-III, Table 4). The one-electron nature of couple-III has been confirmed by differential pulse voltammetric current height. The observed third-step oxidation process possibly arises due to the oxidation of the coordinated ligand moiety (L′) as the next step metal oxidation, i.e. ruthenium(IV) → ruthenium(V) process under non-oxo environment is bit unlikely [44]. However, based on the present data set the possibility of ruthenium(IV) → ruthenium(V) oxidation cannot be exclusively ruled out.

The potential data (Table 4) indicate that the phenanthroline complex (**1b**) is relatively easier to oxidize compared to the bipyridine complex (**1a**).

The bipyridine- and phenanthroline-based reductions of **1a** and **1b**, respectively, are observed at the negative side of SCE. (Table 4, Fig. 4) [41,45].

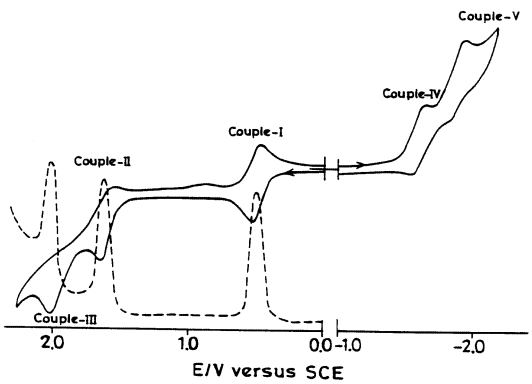

Fig. 4. Cyclic voltammograms of a $\sim 10^{-3}$ M solution of complex **1b** in acetonitrile at 298 K. Differential pulse voltammograms are shown only for positive potentials.

4. Conclusions

We have observed the direct involvement of $Ru(bpy)_2$ and $Ru(phen)_2$ cores in facilitating the cleavage of the N–C bond of the binucleating phenolato diimine function, H_2L, which in other way is found to be fairly stable. The reaction in turn yields ruthenium–bipyridine/phenanthroline heterochelates (**1a** and **1b**) incorporating ketonic imine function, $^{-}OC_6H_4$–$C(CH_3)$=N–H, (L′) having rare –CH=N–H fragment. The complexes exhibit successive one-electron oxidation and reduction processes. Phenanthroline complex (**1b**) is found to be oxidized at a lower potential compared to the bipyridine derivative (**1b**); as far as emission is concerned bipyridine complex (**1a**) seems to be the better choice. Electrochemical as well as chemical oxidations of the complexes lead to the formation of unstable ruthenium(III) congeners at room-temperature.

5. Supplementary material

Crystallographic data for the structural analysis have been deposited with the Cambridge Crystallographic Data Center, CCDC No. 152695 for compound **1a**. Copies of this information may be obtained free of charge from The Director, CCDC, 12 Union Road, Cambridge CB2 1EZ, UK

Acknowledgements

Financial support received from the Department of Science and Technology (DST) and Council of Scientific and Industrial research (CSIR), India, are gratefully acknowledged. We also thank the DST for establishing a National Single Crystal Diffractometer Facility at Indian Institute of Technology, Bombay. Special acknowledgement is made to the Regional Sophisticated Instrumental Center, RSIC, Indian Institute of Technology, Bombay for providing NMR and EPR facilities.

References

[1] P.S. Braterm, Reactions of Coordinated Ligands, Plenum, New York, 1988.
[2] R.A. Sheldon, J.K. Kochi, Metal Catalyzed Oxidations of Organic Compounds, Academic Press, New York, 1981.
[3] E.M. Siegbahn, J. Am. Chem. Soc. 118 (1996) 1487.
[4] R.G. Bergman, Acc. Chem. Res. 117 (1995) 9774.
[5] M. Menon, A. Pramanik, N. Bag, A. Chakravorty, Inorg. Chem. 33 (1994) 433.
[6] S. Murai, F. Kakiuchi, S. Sekine, Y. Tanaka, A. Kamatani, M. Sinoda, N. Chatani, Nature 366 (1993) 529.
[7] C.J. Li, D. Wang, L.D. Chen, J. Am. Chem. Soc. 117 (1995) 12 867.
[8] R.H. Schultz, A.A. Bengali, M.J. Tauber, B.H. Weiller, E.P. Wasserman, K.R. Kyle, C.B. Moore, R.G. Bergman, J. Am. Chem. Soc. 116 (1994) 7369.
[9] B.K. Santra, G.A. Thakur, P. Ghosh, A. Pramanik, G.K. Lahiri, Inorg. Chem. 35 (1996) 3050.
[10] B.K. Santra, G.K. Lahiri, J. Chem. Soc., Dalton Trans. (1997) 129.
[11] B.K. Santra, P. Munshi, G. Das, P. Bharadwaj, G.K. Lahiri, Polyhedron 18 (1999) 617.
[12] B.K. Santra, G.K. Lahiri, J. Chem. Soc., Dalton Trans. (1997) 1883.
[13] B.K. Santra, G.K. Lahiri, J. Chem. Soc., Dalton Trans. (1998) 1613.
[14] A. Bharath, B.K. Santra, P. Munshi, G.K. Lahiri, J. Chem. Soc., Dalton Trans. (1998) 2443.
[15] G.K. Lahiri, S. Goswami, L.R. Falvello, A. Chakravorty, Inorg. Chem. 26 (1987) 3365.
[16] N. Bag, S.B. Choudhury, G.K. Lahiri, A. Chakravorty, J. Chem. Soc., Chem. Commun. (1990) 1626.
[17] N. Bag, S.B. Choudhury, A. Pramanik, G.K. Lahiri, A. Chakravorty, Inorg. Chem. 29 (1990) 5013.
[18] G.K. Lahiri, A.M. Stolzenberg, Angew. Chem., Int. Ed. Engl. 32 (1993) 429.
[19] S. Chakraborty, P. Munshi, M. Walawalkar, G.K. Lahiri, J. Chem. Soc., Dalton Trans. (2000) 2875.
[20] E.C. Johnson, B.P. Sullivan, D.J. Salmon, S.A. Adeyemi, T.J. Meyer, Inorg. Chem. 17 (1978) 2211.
[21] D.T. Sawyer, A. Sobkowiak, J.L. Roberts Jr., Electrochemistry for Chemists, Wiley, New York, 1995.
[22] A.C.T. North, D.C. Phillips, F.S. Mathews, Acta Crystallogr., Sect. A 24 (1968) 351.
[23] G.M. Sheldrick, SHELXTL, Version 5.03, Siemens Analytical X-ray Instruments Inc., Madison, WI, 1994.
[24] S. Chakraborty, P. Munshi, G.K. Lahiri, Polyhedron 18 (1999) 1437.
[25] P. Munshi, R. Samanta, G.K. Lahiri, Polyhedron 17 (1998) 1913.
[26] J.R. Dyer, Application of Absorbtion Spectroscopy of Organic Compounds, Prentice-Hall, New Delhi, 1989 (p. 37).
[27] B.K. Santra, G.K. Lahiri, J. Chem. Soc., Dalton Trans. (1998) 139.
[28] A.M.W. Cargill Thompson, D.A. Bardwell, J.C. Jeffery, M.D. Ward, Inorg. Chim. Acta 267 (1998) 239.
[29] P. Munshi, R. Samanta, G.K. Lahiri, J. Organomet. Chem. 586 (1999) 176.
[30] B.M. Holligan, J.C. Jeffery, M.K. Norgett, E. Schatz, M.D. Ward, J.Chem. Soc., Dalton Trans (1992) 3345.
[31] N. Bag, A. Pramanik, G.K. Lahiri, A. Chakravorty, Inorg. Chem. 31 (1992) 40.
[32] V.R.L. Constantino, H.E. Toma, L.F.C. de Oliveira, F.N. Rein, R.C. Rocha, D.O. Silva, J. Chem. Soc., Dalton Trans (1999) 1735.
[33] K.D. Keerthi, B.K. Santra, G.K. Lahiri, Polyhedron 17 (1998) 1387.
[34] M.H. Kuchama, T. Nicholson, A. Davison, W.M. Davis, A.G. Jones, Inorg. Chem. 36 (1997) 3237.
[35] M.D. Ward, Inorg. Chem. 35 (1996) 1712.
[36] G.A. Crosby, W.H. Elfring Jr., J. Phys. Chem. 80 (1976) 2206.
[37] J.V. Houten, R.J. Watts, J. Am. Chem. Soc. 98 (1976) 4853.
[38] E.F. Godefroi, E.L. Little, J. Org. Chem. 21 (1956) 1163.
[39] P. Chen, R. Duesing, D.K. Graff, T.J. Meyer, J. Phys. Chem. 95 (1991) 5850.

[40] B. Mondal, M.G. Walawalkar, G.K. Lahiri, J. Chem. Soc., Dalton Trans. (2000) 4209.
[41] B.K. Santra, M. Menon, C.K. Pal, G.K. Lahiri, J. Chem. Soc., Dalton Trans. (1997) 1387.
[42] N. Bag, G.K. Lahiri, S. Bhattacharya, L.R. Falvello, A. Chakravorty, Inorg. Chem. 27 (1988) 4396.
[43] G.K. Lahiri, S. Bhattacharya, S. Goswami, A. Chakravorty, J. Chem. Soc., Dalton Trans. (1990) 561.
[44] G.K. Lahiri, S. Bhattacharya, B.K. Ghosh, A. Chakravorty, Inorg. Chem. 26 (1987) 4324.
[45] E.A. Seddon, K.R. Seddon, Chemistry of Ruthenium, Elsevier, Amsterdam, 1984 (p. 414).